Effect of solid properties on slip at a fluid-solid interface

Amir Alizadeh Pahlavan and Jonathan B. Freund*

Mechanical Science and Engineering, University of Illinois at Urbana-Champaign, Urbana, Illinois 61801, USA

(Received 12 August 2010; revised manuscript received 19 December 2010; published 7 February 2011)

The dependence of velocity slip at a liquid–solid interface upon the character of the solid is studied using atomistic simulation methods for Lennard-Jones model systems. The effect of the thermostatting mechanisms, often used in such simulations, is also investigated. The solid atom vibrational frequency is shown not to have a significant effect on the slip length for the range of parameters investigated; however, it is found that application of a thermostat to the fluid changes the slip length at low shear rates and results in an unphysical divergent slip behavior at high shear rates. On the other hand, removing the generated heat through the walls, which is more analogous to a laboratory condition, results in a nonlinearly decreasing slip length with shear rate that asymptotes to the no-slip limit at high shear rates. This effect is due to viscous heating, which increases the fluid temperature and pressure. A nonlinear relationship between the slip length and the shear rate collapses the shear-rate–slip-length dependence onto a single curve for a range of cases when heat is more realistically removed through the walls.

DOI: 10.1103/PhysRevE.83.021602 PACS number(s): 68.08.−p, 66.20.−d

I. INTRODUCTION

The no-slip condition is clearly a good model in most circumstances where a fluid meets a solid boundary, but significant slip has been observed at high shear rates and has been proposed as a model in circumstances when the no-slip boundary condition leads to singular or unphysical behaviors [1–8]. The slip behavior has been shown to be dependent on the liquid–solid interaction energy and the commensurability of the liquid and solid atoms [6,9]. In general, as the substrate-induced liquid ordering near the wall increases, the momentum transfer between the liquid and solid is enhanced and consequently the slip length decreases [9–11]. Hence, special attention should be paid to the details of fluid–solid interfaces when dealing with such systems.

Studies of slip using molecular dynamics simulations (MD) can be categorized based upon the wall model and thermostatting procedure used. In one of the first systematic MD studies, Thompson *et al.* [12] investigated slip in a Lennard-Jones liquid between solid walls and found that slip is directly related to the amount of structure induced in the fluid by the walls. They constructed their flexible wall model from atoms attached to their lattice sites with springs, whereby the linear spring stiffness controls the thermal roughness of the wall and its responsiveness to the fluid. A Langevin thermostat was applied to the fluid and it was claimed that velocity profiles were insensitive to the thermostat. This approach has become the common practice [9,13–15].

The effect of wall stiffness on slip has also been investigated [16,17]. Jabbarzadeh *et al.* [16] studied a Couette flow of hexadecane molecules and observed that, with decreasing wall stiffness, the interactions of fluid and solid atoms increase and consequently the slip length decreases. Priezjev [17] has also analyzed the effect of wall stiffness on the slip length and observed that the shear-rate dependence weakens for softer walls. However, the effect of wall stiffness on the slip length is complex and not yet well understood. It seems that decreasing the wall stiffness can reduce the slip length by facilitating greater penetration of solid atoms into the fluid, which is expected to increase momentum transport, but it might also decrease the surface-induced structuring of the near-wall fluid atoms and thereby increase the slip length [12,17].

The temperature dependence of slip length has also been studied [15,18–20]. However, there does not appear to be a complete study of the effects of how temperatures are set and maintained by so-called thermostatting techniques in such simulations. Heinbuch and Fischer [21] studied the flow of a Lennard-Jones liquid through a cylindrical pore and found that the velocity profiles were sensitive to the heat removal mechanisms. Liem *et al.* [22] compared different methods for forming wall boundaries and controlling temperature and concluded that "a fluid shearing with heat being removed at a rate, which is naturally realizable either through conduction or homogeneously, behaves in much the same way." However, Padilla *et al.* [23] showed that for the high shear rates usually selected for MD simulations to accelerate statistical convergence, heat is eliminated by the thermostat at rates that are higher than the rate of transport of heat by conduction within the fluid. Moreover, there can be inadequate time in such cases to maintain equipartition of energy, so the statistics will depend on which degrees of freedom are coupled with the thermostat. Later, Khare *et al.* [24] compared two different thermostatting mechanisms (thermostatting the fluid and thermostatting just the solid) and observed differences in how viscosity depends upon shear rate. Our simulations are designed to fully study these issues in a well-defined model system.

The shear dependence of slip length has been the subject of several studies. Thompson and Troian [13] studied the effect of shear rate on the slip length and found a power law dependence. They observed that at sufficiently low shear rates, the slip condition is consistent with the Navier model; however, at higher shear rates, the Navier condition fails and slip length increases in a nonlinear fashion, apparently unboundedly, beyond a critical shear rate, even though the liquid is still Newtonian at these same shear rates. A similar shear-rate dependence is also reported in sheared simple liquids [9,25]

*jbfreund@illinois.edu; also Aerospace Engineering

and polymer films [14]. Priezjev [15,17] later found that the growth of slip length with shear rate is dependent on the wall–fluid interaction and wall stiffness. He reported a transition from nonlinear to linear shear-rate dependence as wall–fluid interaction becomes stronger [15]. He also found that the shear-rate dependence weakens as the wall stiffness decreases [17]. Niavarani and Priezjev [26] also investigated the shear-rate dependence of slip in polymer melts and observed that as shear increases, the slip length has a local minimum before rapidly increasing.

Recently, Martini *et al.* [27,28] studied slip in a Couette flow of *n*-decane molecules, and observed that slip length asymptotes to a constant value at high shear rates. As they explained, the general belief is that as the speed of fluid atoms increases, the effective surface roughness decreases, and hence the resistance to slip vanishes; however, in practice, the momentum transfer between solid and fluid due to collisions seems to increase as the speed of fluid atoms increases. Martini *et al.* [28] argued that those who have observed unbounded slip at high shear rates used a rigid wall model, while using a flexible wall model results in a bounded slip. A rigid wall cannot conduct heat out of the fluid, so by using such a wall it was necessary to thermostat the fluid to remove the generated heat. For cases with flexible walls, they applied the thermostat just to the solid. Thus the effects of the thermostat and the wall properties could not be completely decoupled.

Our atomistic simulations in a Couette flow geometry are designed to directly address the effect of wall model and thermostatting mechanism on slip as quantified by the slip length. The simulation methods and the thermostatting mechanisms used in this work are introduced in Secs. II and III, respectively. Our simulation results are presented and compared with the previous predictions in Sec. IV. The oscillation frequency of solid atoms is shown not to have a considerable direct effect on the slip length, especially if compared to the effect of temperature. It is then shown that both the temperature change and the resulting pressure change are responsible for the observed variations in slip length. Regarding the importance of these factors, we then analyze the effect of different thermostatting mechanisms on slip. It is observed that different common thermostatting procedures can result in drastically different slip behaviors, especially at high shear rates, while the slip length is found not to be very sensitive to the oscillation frequency of the solid atoms. Finally, a nonlinear relationship for slip length versus shear rate is proposed for the realistic case of removing the generated heat through the channel walls.

II. SIMULATION METHODS

Our system is entirely constructed of Lennard-Jones atoms, which interact via the truncated pair potential

$$U_{ij} = \begin{cases} 4\epsilon_{ij}\left[\left(\frac{\sigma_{ij}}{r_{ij}}\right)^{12} - \left(\frac{\sigma_{ij}}{r_{ij}}\right)^{6}\right] & \text{if} \quad r_{ij} < r_c \\ 0 & \text{if} \quad r_{ij} > r_c, \end{cases} \tag{1}$$

where ϵ_{ij} is the energy of an interaction between atoms of type i and j, and the Lennard-Jones length scale is σ_{ij}, which corresponds to a zero-force radius of $r_0 = 2^{1/6}\sigma_{ij}$. All atomic interactions are assumed to have the same $\sigma_{ij} = \sigma$. The

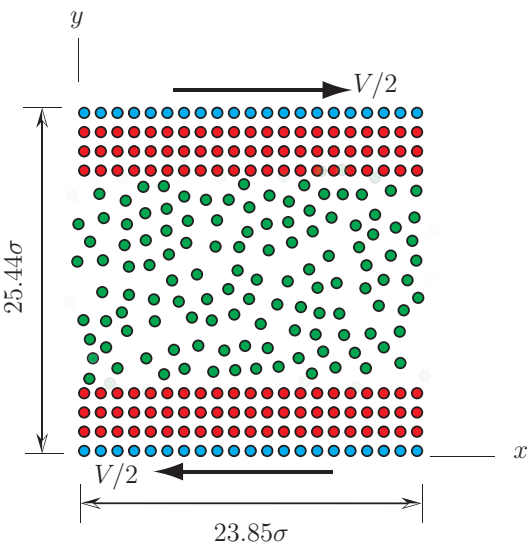

FIG. 1. (Color online) Schematic of the simulation domain. The domain also extends 7.94σ in the z direction.

standard cutoff radius of $r_c = 2.5\sigma$ is selected to reduce the computational cost as is commonly done [3,29]. Most fluid properties, including viscosity, which is particularly relevant in the present study, are insensitive to r_c for $r_c > 2.5\sigma$ [29–31].

We simulate 2994 fluid atoms flowing between parallel crystal walls, each containing 600 atoms. Each wall consists of four layers of a face-centered cubic (FCC) lattice with a [001] plane forming the interface with the liquid. The atoms in the bottom layer of each wall have positions fixed to maintain the integrity of the wall. The walls move at speeds $\pm V/2$ along the x axis to create the shear flow (see Fig. 1). In most of the simulations, the size of the domain is $L_x \times L_y \times L_z = 23.85\sigma \times 25.44\sigma \times 7.94\sigma$, and periodic boundary conditions are enforced in the x and z directions. The height L_y changes slightly in the constant pressure case. The wall atoms in our baseline case have $m_s = 10m_f$ and $\epsilon_{ss} = 10\epsilon_{ff}$ to give this model material a high melting temperature. The choice of these parameters results in a matched fluid–solid oscillation frequency ($\omega_s = \sqrt{\epsilon_{ss}/m_s} = \sqrt{\epsilon_{ff}/m_f} = \omega_f$), which should promote thermal transport. Such a combination has been successfully used before by Freund [32] to make the wall stiff without introducing a short time scale into the simulations. To compare our solid wall properties with those of previous studies (e.g., Priezjev [17] or Asproulis and Drikakis [33]), we track the trajectory of wall atoms in contact with fluid atoms to compute an effective spring stiffness coefficient of the wall atoms $k_{\text{eff}} = 3k_BT/\langle\delta u^2\rangle$, in which k_B is the Boltzmann constant and $\langle\delta u^2\rangle$ is the mean square displacement of the atoms. In our simulations k_{eff} varies from around 100 to $500\epsilon/\sigma^2$ ($\epsilon = \epsilon_{ff}$), and the oscillation period of the wall atoms $T = 2\pi\sqrt{m_s/k_{\text{eff}}}$ ranges from 0.7 to 1.2τ ($\tau = \sqrt{m_f\sigma^2/\epsilon_{ff}}$), which is much larger than the integration time step 0.0046τ. Our choice of parameters ensures that the Lindemann criterion for melting is satisfied: $\langle\delta u^2\rangle/d^2 \leqslant 0.023$. The fluid–solid interaction energy is $\epsilon_{fs} = 0.1\epsilon_{ff}$, which could be considered nonwetting with an anticipated contact angle of $\theta = \cos^{-1}(2\epsilon_{fs}/\epsilon_{ff} - 1) \approx 143^\circ$.

The equation of motion is integrated in time using the standard second-order velocity-Verlet algorithm with a numerical time step of $\Delta t = 0.0046\tau$. Parameters for argon would correspond to $\sigma = 3.4\text{Å}$, $\epsilon/k_B = 120\text{K}$, $m = 6.69 \times 10^{-23}\text{g}$, and $\tau = 2.161 \times 10^{-12}\text{s}$. [1,3,9] The mean temperature, density, and velocity were monitored to establish when the system became statistically stationary. It was deemed stationary when the mean profiles did not deviate beyond 1% over 10^5 time steps, which was achieved after 10^6 time steps. Statistics were accumulated in several ensembles over the next 50 to 70×10^6 time steps with data collected in bins of height $\Delta y = 0.05\sigma$. The nominal fitting error R in calculating the slip length for the lowest shear rate, where R^2 is minimized in the linear least square fit of the velocity profile, is approximately 0.03σ, while for the highest shear rates, this error decreases by an order of magnitude, reaching approximately 0.002σ.

III. THERMOSTATTING PROCEDURES

The wall temperature T_s is maintained with the thermostat proposed by Anderson [34]. In this method, at the end of each time step there is a finite probability for each atom in the thermostated region to be assigned a new velocity randomly selected from the Boltzmann distribution for the target temperature. It is applied only to the (nonfixed) solid layer farthest from the fluid–solid interface, and its probability of velocity reassignment is set to be $\nu = 0.005$. Reducing the reassignment probability to $\nu = 0.002$ showed no appreciable effect on the wall temperature or slip lengths and hence alters none of our conclusions. Following Xue *et al.* [35,36], we chose $T_s = 0.71\epsilon/k_B$ and $\rho = 0.84\sigma^{-3}$ as our base state; this combination represents a generic liquid near its triple point and allows us to investigate a wide range of shear rates with fluid temperature less than its critical value [35–37].

In one set of simulations, a Langevin thermostat [38] is also applied to the fluid atoms to compare our results with those published for similarly thermostated fluids. As Evans and Morris [39] pointed out, using thermostats that assume a predetermined velocity profile can yield spurious results. They recommended using profile-unbiased thermostats, particularly at high shear rates. Hence, in this case, only the equation of motion in the z direction (perpendicular to the shear plane) is augmented to be

$$m\ddot{z}_i = -\sum_{i \neq j} \frac{\partial U_{ij}}{\partial z_i} - m\Gamma \frac{dz_i}{dt} + F_i(t). \tag{2}$$

The final two terms on the right lead to isothermal fluid conditions by weakly coupling the particle dynamics to a nominal Langevin thermal reservoir. The friction coefficient Γ regulates the heat flux from the system and F_i is a Gaussian random force with zero mean and variance $2m\Gamma k_B T\delta(t)$, where T is the target fluid temperature, $\delta(t)$ is the Dirac symbol, and k_B is the Boltzmann constant. We set $\Gamma = 1.0\tau^{-1}$, which is commonly used. This value is claimed to be large enough to remove heat from the system without inducing substantial changes in temperature, but is thought to be small enough to minimize disturbances to the particle trajectories [9,12,13,38].

IV. RESULTS AND DISCUSSION

A. Slip dependence on physical parameters

First, we investigate the effect of the solid atom linear vibrational frequency on the slip length. We change the vibrational frequency and amplitude by altering the atomic mass and interaction energy. Since our baseline simulation has a matched fluid–solid oscillation frequency, changing the mass of the solid atoms results in a frequency mismatch. This, in turn, increases the interface resistance, the so-called Kapitza resistance [40]. Higher Kapitza resistance increases the temperature jump at fluid–solid interface and thus leads to a higher fluid temperature.

As seen in Fig. 2(a), increasing the mass of the solid atoms by a factor of 16 results in a larger temperature jump at the fluid–solid boundary. Along with this, there is also a more distinct quasicrystalline layering of the near-wall fluid atoms and a moderate decrease in the slip length [Figs. 2(b) and 2(c)]. We have observed essentially the same effects in a wide range of solid atom oscillation frequencies when changing the mass or interaction energy. However, it is as yet unclear whether these effects derived directly from the oscillation frequency mismatch or indirectly via the increased fluid temperature. To investigate this, we fixed the mass of the solid atoms at $m_s = 10m_f$ and increased the target temperature for the wall thermostat so that the fluid temperature matches that of the $m_s = 160m_f$ case [Fig. 2(a)]. Comparing the density and the velocity profiles of these two cases [Figs. 2(b) and 2(c)], we find that they are nearly identical. This indicates that when viscous heating is substantial, as it is in most MD simulations of shear flows, it is the increased temperature brought about via changes in Kapitza resistance that overwhelms any direct effect of the vibrational frequency on the slip length. Reducing the overall shear rate by a factor of 4 suppresses viscous heating and significantly reduces the temperature difference brought about by the Kapitza resistance. In this case, the slip length and the density profiles are essentially independent of the wall properties (not shown because no changes were observed).

As temperature increases at fixed volume it causes the fluid pressure to increase as well, and we next isolate these two effects. Pressure is regulated by leaving the top wall in the simulation unconstrained and applying the required negative y-directed force uniformly to the top layer of wall atoms [41]. This wall is then fixed at its mean vertical position as statistics are accumulated. Increasing the temperature at fixed pressure, the fluid volume and the channel height increase accordingly. With the fluid less confined at fixed pressure we might expect slip to increase, but, as in most viscosity constitutive models, temperature seems to be more important. Figure 3(a) shows that the slip length continues to decrease with temperature, following a nearly linear trend. This behavior shows the direct influence of temperature on slip length and might be attributed to the fact that as the kinetic energy of atoms increases with temperature, the momentum transfer because of collisions also becomes enhanced, therefore decreasing the slip length. As Fig. 3(b) shows, increasing the pressure causes the slip length to substantially decrease. Such a dependence of the slip length on pressure has been reported by Barrat and Bocquet [11]. However, they used fixed solid atoms in their wall model and consequently had to thermostat the fluid to remove the

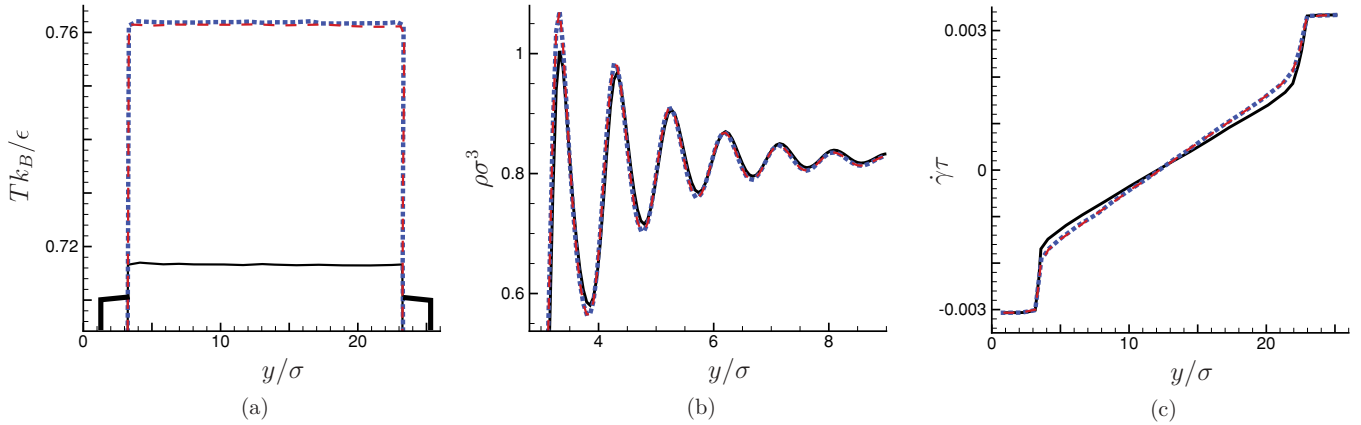

FIG. 2. (Color online) The effect of increasing mass and temperature on the fluid (a) temperature, (b) density, and (c) velocity profiles for $V = 0.006\dot{\gamma}\tau$;—— $T_s = 0.71\epsilon/k_B$ and $m_s = 10m_f$; - - - - $T_s = 0.71\epsilon/k_B$ and $m_s = 160m_f$; and - - - - - - - $T_s = 0.75\epsilon/k_B$ and $m_s = 10m_f$. The thick line ——— shows the wall temperature.

generated heat. Assuming that the viscosity increases with pressure, the wall-fluid friction coefficient, defined as shear viscosity to slip length ratio, should also increase.

B. Slip dependence on the thermostatting procedure

Seeing the sensitivity of slip to temperature and pressure, it is important to assess what, if any, role the numerical thermostats used in the simulations to regulate temperature might play. The most common practice in such simulation studies of slip is to apply a Langevin thermostat to the fluid atoms [9,12,13,38]. The thermostat is applied in the direction perpendicular to the shear plane to avoid bias in the flow direction. However, as discussed earlier, a few studies suggest that such an application of a thermostat would affect the flow behavior [23,24].

We perform two sets of simulations to assess this. Case A has been discussed up to this point. An Anderson thermostat is applied just to the solid layer farthest from the fluid–solid interface. This was done specifically to minimize the influence of the thermostat, which is fundamentally unphysical. In case B, an additional Langevin thermostat is applied to the fluid atoms.

We showed [Fig. 3(a)] that the slip length is sensitive to the temperature. To distinguish the effects of temperature from any direct effect of the thermostat, we set the Langevin thermostat applied in the B cases to target the temperature observed in the A cases. Thus, the fluid temperatures will be the same and any differences between the cases can be considered a direct (and presumably unphysical) influence of the thermostat. However, it should be noted that such a procedure is only possible for low shear rates, in which the viscous heating is not considerable and the fluid temperature profile observed in the A cases is nearly flat.

At low shear rates, we expect any differences between the A and B cases to be relatively small since viscous heating is small and the thermostat in this limit alters the atomic velocities only a small amount to maintain the target temperature. At the lowest shear rate simulated, $\dot{\gamma}\tau = 0.0015$, the predicted slip length of case A is $L_s/\sigma = 8.5$, while that of case B for $\Gamma = 1$ and $10\tau^{-1}$ are respectively $L_s/\sigma = 7.9$ and 7.2. Therefore, for low shear rates ($\dot{\gamma}\tau = 0.0015$ to 0.006) in which the viscous heating is not considerable, application of the thermostat to the fluid changes the slip length by 10–20% . This difference is expected to increase substantially at high shear rates in which the viscous heating becomes more significant.

To compare our results with those reported for slip at high shear rates, we fix the fluid temperature of case B

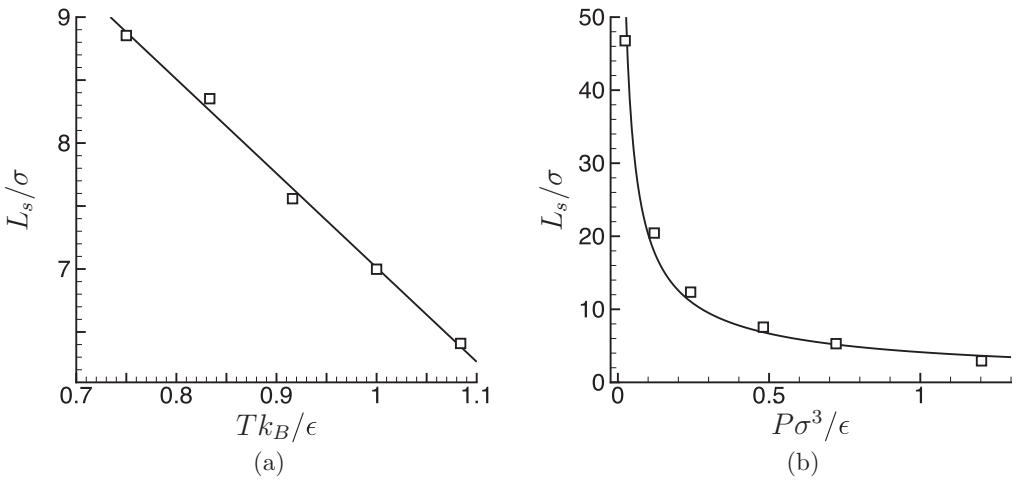

FIG. 3. Slip length dependence on (a) temperature at constant pressure $P = 0.48\epsilon/\sigma^3$ with linear fit $L_s/\sigma = 14.34 - 7.3T$ and (b) pressure at constant temperature $T_s = 0.83\epsilon/k_B$, $\dot{\gamma}\tau = 0.006$ with power fit $L_s/\sigma = 5P^{-0.6}$.

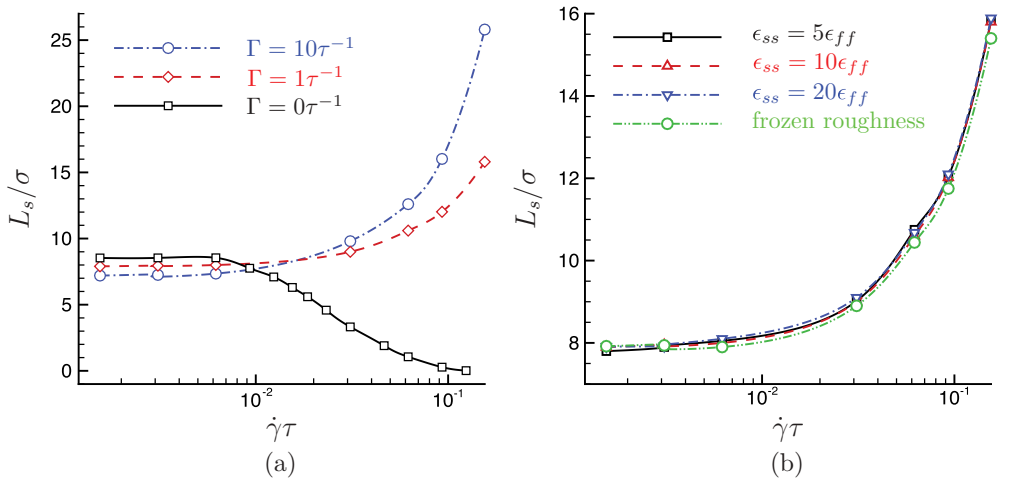

FIG. 4. (Color online) The effect of (a) thermostatting mechanism and (b) wall parameters on the slip length versus shear-rate behavior.

at $T = 0.72\epsilon/k_B$, which matches the fluid temperature of case A at low shear rates. Moreover, since the dynamics of fluid molecules is affected by Γ [42], we report results using both $\Gamma = 1$ and $10\tau^{-1}$ to support our conclusions. As Fig. 4(a) shows, the predicted slip length of the A and B cases start diverging for $\dot{\gamma}\tau \gtrsim 0.01$; it should be noted that for high shear rates, the A and B cases are not at equivalent thermodynamic states. At lower shear rates, increasing Γ decreases the predicted slip length; however, at higher shear rates, in which the viscous heating becomes substantial, increasing Γ eliminates the generated heat more quickly and increases the predicted slip length. The rapid increase of slip length with shear rate we see for the fluid-thermostated case B is consistent with several studies that employed a thermostat for the fluid [9,13,14,25]. However, more recently, Martini *et al.* [27,28] observed a contradictory behavior at high shear rates. Simulating *n*-decane, they reported that the slip length increases seemingly without bound when the atomic wall is perfectly rigid and heat is removed by thermostatting the fluid while the slip length asymptotes to a constant value when a flexible wall model is used and the heat is removed through the walls. This is consistent with our observations that thermostatting the fluid changes the slip behavior. Our results show that it is the fluid thermostat and not the perfect rigidity of the wall that leads to the rapid increase in slip length. In fact, at low shear rates we observed that the dynamics of the wall atoms do not greatly affect slip in a direct manner [see Fig. 2(c)].

To further investigate this, we extend the simulations of case B to include the effect of changes in the vibrational frequency of the solid atoms. As Fig. 4(b) shows, the slip length increases in the same seemingly unbounded fashion for all the ω_s. This indicates that the effect of vibrational frequency of solid atoms on the slip behavior is not appreciable, even at high shear rates. Therefore, the large slip length at high shear rates is not a direct consequence of wall model used.

For the rough wall case shown in Fig. 4(b), the wall was constructed by fixing an instance of the thermally vibrating wall atoms in the absence of the imposed flow and then collecting flow statistics. This case further shows insensitivity to wall conditions.

For the wall thermostated cases (case A), higher shear rates lead to higher temperatures and higher fluid layering near the walls (see Fig. 5), while the fluid temperature and layering remain unchanged for the B cases (not shown). Given the

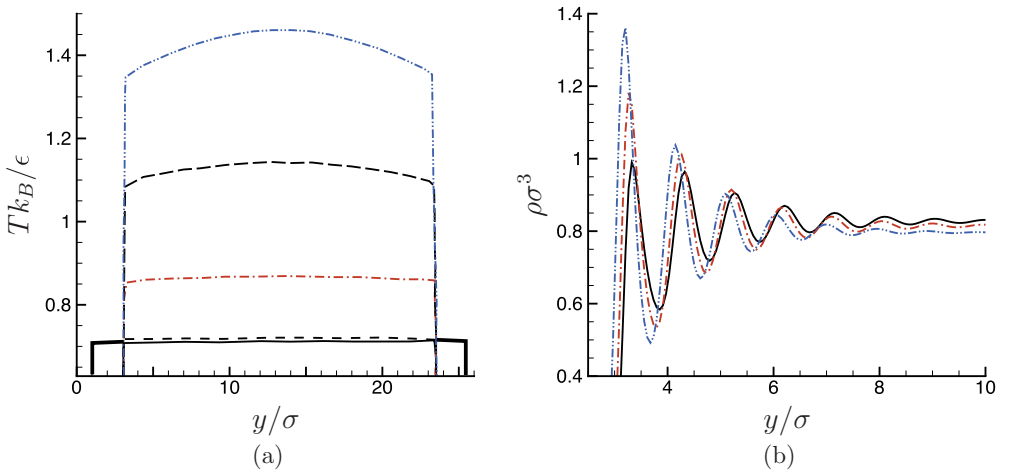

FIG. 5. (Color online) The effect of increasing shear rate on the fluid (a) temperature, (b) density: —— $\dot{\gamma}\tau = 0.0015$; – – – – $\dot{\gamma}\tau = 0.006$; – – – $\dot{\gamma}\tau = 0.031$; – – – $\dot{\gamma}\tau = 0.062$; and– – – – $\dot{\gamma}\tau = 0.093$. The thick line ——— shows the wall temperature.

decreasing slip with increasing temperature seen in Fig. 3(a), it is expected that the increase of temperature is at least partially responsible for the high-shear-rate behavior we observe. It should be noted that the temperature is relatively high at these highest shear rates of the A cases. Such high shear rates and temperatures might not be realistic in thin liquid films; we consider them primarily to analyze the effect of thermostatting as commonly used in MD studies. The critical temperature for Lennard-Jones fluids is $1.35\epsilon/k_B$, so shear heating in the highest shear-rate cases is indeed significant. It is thus not too surprising that the case B fluid thermostat, which was strong enough to remove all this heat, was capable of substantively affecting the dynamics.

It should be noted that at high shear rates with so much viscous heating, an obvious temperature jump forms on the fluid–solid interface, which might also contribute to the behavior we observe for the velocity slip. The temperature jump (ΔT) at the interface can be related to the wall normal heat flux q as $\Delta T = -R_k q$, where R_k is the Kapitza resistance, which is known to be temperature dependent [40,43]. Assuming that the Fourier law is valid, the Kapitza length is defined analogously to the slip length as $L_k = \lambda R_k$, where λ is the thermal conductivity. With this definition, the Kapitza length is the thickness of liquid that would have the same thermal resistance as the interface. Kapitza resistance and velocity slip are believed to be interdependent [4,8,40,43,44]. For example, Khare *et al.* [44] observed that a finite Kapitza length is present in sheared fluids even when the velocity slip is negligible, however, they found that the velocity slip enhances the thermal slip. In our study, at high shear rates with no fluid thermostatting, the temperature jump at the interfaces is obvious. Assuming that the thermal conductivity and the heat flux are almost constant, we conclude that the Kapitza length increases with shear rate while the velocity slip decreases. However, how the temperature jump at the interfaces affects the velocity slip is not yet clear.

C. Slip lengths

The slip behavior initially reported by Thompson and Troian [13] and later by others [9,14,25] obeys the Navier slip condition for low shear rates; but, as shear rate increases the slip length is nonlinearly divergent. As they mentioned, this onset of nonlinear behavior is surprising since the liquid is still Newtonian. Our results on slip length also start with a shear independent region for lower shear rates and as shear rates increases, the Navier slip model breaks down and the slip length decreases nonlinearly until the no slip condition is recovered.

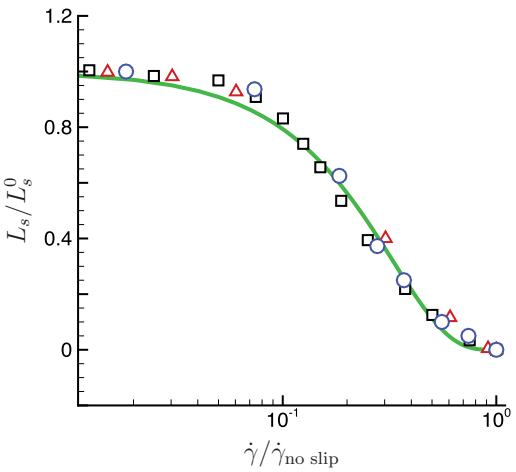

FIG. 6. (Color online) Fit of the slip length: □ $\epsilon_{fs} = 0.1$; Δ $\epsilon_{fs} = 0.2$; ○ $\epsilon_{fs} = 0.3$; and ——— the fit (3).

TABLE I. Asymptotic values corresponding to Fig. 6.

ϵ_{fs}	$\dot{\gamma}_{\text{no slip}}$	L_s^0
0.1	$0.12\tau^{-1}$	8.5σ
0.2	$0.09\tau^{-1}$	4.8σ
0.3	$0.08\tau^{-1}$	2.2σ

Scaling L_s by its limiting value at low shear rates L_s^0 and the shear rate $\dot{\gamma}$ by its value corresponding to the no-slip limit $\dot{\gamma}_{\text{noslip}}$ collapses the data onto the curve shown in Fig. 6. This curve is well fitted by

$$L_s = L_s^0 \left[1 - \left(\frac{\dot{\gamma}}{\dot{\gamma}_{\text{no slip}}}\right)^{\alpha}\right]^{\beta}, \tag{3}$$

with $\alpha = 1.25$ and $\beta = 4$. Our results indicate that both $\dot{\gamma}_{\text{noslip}}$ and L_s^0 decrease as ϵ_{fs} increases. Table I shows the asymptotic values corresponding to Fig. 6.

It should be noted that the magnitude of the slip lengths reported in the case without thermostatting the fluid may depend on the system size. In fact, as the system size increases, the fluid temperature will be higher for the same shear rates and this would, in turn, affect the slip length. However, we expect the reported trend in Fig. 6 to remain unchanged with the channel width in the finite system sizes of typical MD studies. Moreover, as is discussed by Cieplak *et al.* [4], the behavior of slip length is expected to be independent of the flow type. For the same central fluid density, the slip length is expected to behave in much the same way in both Couette and Poiseuille flows.

V. CONCLUSION

In contrast to some studies on the friction of solid–solid [45,46] and fluid–solid interfaces [16,17], we found that the vibrational frequency mismatch does not have an appreciable direct effect on the slip length for our simple materials. However, the atomic mismatch can affect the slip length indirectly through increasing the Kapitza resistance and therefore increasing the fluid temperature as a result of less efficient heat transfer into the walls. In a fixed volume system, the pressure increases with the temperature; therefore, to understand which of these two factors is responsible for the observed decrease in slip length, we performed simulations isolating the effect of each. We found that increasing temperature and pressure both decreases the slip length.

At low shear rates, a standard-strength fluid thermostat (case A) was shown to change the slip length by up to 20% . As shear rate increases, it becomes impossible to isolate the effect of thermostatting mechanisms on the slip length; however, we found that applying the thermostat to the fluid leads to the

apparently divergent slip lengths at high shear rates. Therefore, at high shear rates, the thermostatting mechanism often applied in atomistic simulations to control temperatures is shown to have a direct effect on slip. Additional simulations showed that it is not the oscillation frequency of solid atoms that is responsible for the unbounded slip length at high shear rates, but the application of the thermostat to the fluid. Indeed, using a perfectly rigid wall, one has no choice but to apply the thermostat to the fluid, which leads to unrealistic slip lengths.

Removing the heat in a realistic manner through the walls, we observed a decreasing slip with shear rate that asymptotes to the no-slip limit at high shear rates. This behavior can be attributed to the increase in the fluid temperature and pressure as a result. In fact, as the rate of viscous heating increases beyond the rate at which the system conducts the heat through the walls, the fluid temperature increases and becomes parabolic with its maximum at the centerline of the channel. The fluid layering near the walls also increases with shear rate for case A, while it remains unchanged for case B.

Finally, based on our data we suggest a general nonlinear relationship for slip length in the form of $L_s = L_s^0[1 - (\dot{\gamma}/\dot{\gamma}_{\text{no slip}})^{\alpha}]^{\beta}$ for the case of heat being realistically removed through the walls. The well-known linear Navier slip boundary condition is the low shear limit of this relationship.

ACKNOWLEDGMENTS

We thank Adam M. Willis for fruitful discussion early on in this work. Funding from the National Science Foundation is gratefully acknowledged (Grant No. CTS-0245642).

[1] J. Koplik, J. R. Banavar, and J. F. Willemsen, Phys. Fluids A **1**, 781 (1989).
[2] J. Koplik and J. R. Banavar, Phys. Fluids **7**, 3118 (1995).
[3] J. Koplik and J. R. Banavar, Annu. Rev. Fluid Mech. **27**, 257 (1995).
[4] M. Cieplak, J. Koplik, and J. R. Banavar, Phys. Rev. Lett. **86**, 803 (2001).
[5] S. Granick, Y. Zhu, and H. Lee, Nature Mat. **2**, 221 (2003).
[6] E. Lauga, M. P. Brenner, and H. A. Stone, in *Handbook of Experimental Fluid Dynamics* (Springer, New York, 2005), Chap. 15.
[7] C. Neto, D. R. Evans, E. Bonaccurso, H. J. Butt, and V. S. J. Craig, Rep. Prog. Phys. **68**, 2859 (2005).
[8] L. Bocquet and J.-L. Barrat, Soft Matter **3**, 685 (2007).
[9] N. V. Priezjev and S. M. Troian, J. Fluid Mech. **554**, 25 (2006).
[10] L. Bocquet and J.-L. Barrat, Phys. Rev. E **49**, 3079 (1994).
[11] J.-L. Barrat and L. Bocquet, Phys. Rev. Lett. **82**, 4671 (1999).
[12] P. A. Thompson and M. O. Robbins, Phys. Rev. A **41**, 6830 (1990).
[13] P. A. Thompson and S. M. Troian, Nature (London) **389**, 360 (1997).
[14] N. V. Priezjev and S. M. Troian, Phys. Rev. Lett. **92**, 018302 (2004).
[15] N. V. Priezjev, Phys. Rev. E **75**, 051605 (2007).
[16] A. Jabbarzadeh, J. D. Atkinson, and R. I. Tanner, J. Chem. Phys. **110**, 2612 (1999).
[17] N. V. Priezjev, J. Chem. Phys. **127**, 144708 (2007).
[18] Z. Guo, T. S. Zhao, and Y. Shi, Phys. Rev. E **72**, 036301 (2005).
[19] S. Lichter, A. Martini, R. Q. Snurr, and Q. Wang, Phys. Rev. Lett. **98**, 226001 (2007).
[20] J. Servantie and M. Müller, Phys. Rev. Lett. **101**, 026101 (2008).
[21] U. Heinbuch and J. Fischer, Phys. Rev. A **40**, 1144 (1989).
[22] S. Y. Liem, D. Brown, and J. H. R. Clarke, Phys. Rev. A **45**, 3706 (1992).
[23] P. Padilla and S. Toxvaerd, J. Chem. Phys. **104**, 5956 (1996).
[24] R. Khare, J. de Pablo, and A. Yethiraj, J. Chem. Phys. **107**, 2589 (1997).
[25] R. S. Voronov, D. V. Papavassiliou, and L. L. Lee, J. Chem. Phys. **124**, 204701 (2006).
[26] A. Niavarani and N. V. Priezjev, Phys. Rev. E **77**, 041606 (2008).
[27] A. Martini, A. Roxin, R. Q. Snurr, Q. Wang, and S. Lichter, J. Fluid Mech. **600**, 257 (2008).
[28] A. Martini, H.-Y. Hsu, N. A. Patankar, and S. Lichter, Phys. Rev. Lett. **100**, 206001 (2008).
[29] D. Frenkel and B. Smit, *Understanding Molecular Simulation* (Academic, New York, 1996).
[30] M. P. Allen and D. J. Tildesley, *Computer Simulation of Liquids* (Clarendon, Oxford, 1987).
[31] A. Trokhymchuk and J. Alejandre, J. Chem. Phys. **111**, 8510 (1999).
[32] J. B. Freund, Phys. Fluids **17**, 022104 (2005).
[33] N. Asproulis and D. Drikakis, Phys. Rev. E **81**, 061503 (2010).
[34] H. C. Andersen, J. Chem. Phys. **72**, 2384 (1980).
[35] L. Xue, P. Keblinski, S. R. Phillpot, S. U.-S. Choi, and J. A. Eastman, J. Chem. Phys. **118**, 337 (2003).
[36] L. Xue, P. Keblinski, S. R. Phillpot, S. U.-S. Choi, and J. A. Eastman, Int. J. Heat Mass Transf. **47**, 4277 (2004).
[37] R. Vogelsang, C. Hoheisel, and G. Ciccotti, J. Chem. Phys. **86**, 6371 (1987).
[38] G. S. Grest and K. Kremer, Phys. Rev. A **33**, 3628 (1986).
[39] D. J. Evans and G. P. Morriss, Phys. Rev. Lett. **56**, 2172 (1986).
[40] J.-L. Barrat and F. Chiaruttini, Mol. Phys. **101**, 1605 (2003).
[41] J. B. Freund, J. Chem. Phys. **116**, 2194 (2002).
[42] M. Tsige and G. S. Grest, J. Chem. Phys. **120**, 2989 (2004).
[43] B. H. Kim, A. Beskok, and T. Cagin, J. Chem. Phys. **129**, 174701 (2008).
[44] R. Khare, P. Keblinski, and A. Yethiraj, Int. J. Heat Mass Transf. **49**, 3401 (2006).
[45] M. R. Sorensen, K. W. Jacobsen, and P. Stoltze, Phys. Rev. B **53**, 2101 (1996).
[46] R. J. Cannara, M. J. Brukman, K. Cimatu, A. V. Sumant, S. Baldelli, and R. W. Carpick, Science **318**, 780 (2007).